

H. Amthauer  
T. Denecke  
T. Rohlfsing  
J. Ruf  
M. Böhmig  
M. Gutberlet  
U. Plöckinger  
R. Felix  
A. J. Lemke

## Value of image fusion using single photon emission computed tomography with integrated low dose computed tomography in comparison with a retrospective voxel-based method in neuroendocrine tumours

Received: 29 August 2004  
Revised: 2 November 2004  
Accepted: 9 November 2004  
Published online: 31 December 2004  
© Springer-Verlag 2004

H. Amthauer (✉) · T. Denecke ·  
J. Ruf · M. Gutberlet · R. Felix ·  
A. J. Lemke  
Klinik für Strahlenheilkunde,  
Campus Virchow-Klinikum,  
Charité-Universitätsmedizin Berlin,  
Augustenburger Platz 1,  
13353 Berlin, Germany  
e-mail: h.amthauer@charite.de  
Tel.: +49-30-450557013  
Fax: +49-30-450557909

T. Rohlfsing  
Department of Neurosurgery,  
Image Guidance Laboratories,  
Stanford University,  
Stanford, CA, USA

M. Böhmig · U. Plöckinger  
Medizinische Klinik m.S. Hepatologie  
und Gastroenterologie,  
Interdisziplinäres Stoffwechsel-  
Centrum, Campus Virchow-Klinikum,  
Charité-Universitätsmedizin Berlin,  
Berlin, Germany

**Abstract** The objective was the evaluation of single photon emission computed tomography (SPECT) with integrated low dose computed tomography (CT) in comparison with a retrospective fusion of SPECT and high-resolution CT and a side-by-side analysis for lesion localisation in patients with neuroendocrine tumours. Twenty-seven patients were examined by multidetector CT. Additionally, as part of somatostatin receptor scintigraphy (SRS), an integrated SPECT–CT was performed. SPECT and CT data were fused using software with a registration algorithm based on normalised mutual information. The reliability of the topographic assignment of lesions in SPECT–CT, retrospective fusion and side-by-side analysis was evaluated by two blinded readers. Two patients were not enrolled in the final analysis because of misregistrations in the retrospective fusion. Eighty-seven foci were included in the analysis. For the anatomical assignment of foci,

SPECT–CT and retrospective fusion revealed overall accuracies of 91 and 94% (side-by-side analysis 86%). The correct identification of foci as lymph node manifestations ( $n=25$ ) was more accurate by retrospective fusion (88%) than from SPECT–CT images (76%) or by side-by-side analysis (60%). Both modalities of image fusion appear to be well suited for the localisation of SRS foci and are superior to side-by-side analysis of non-fused images especially concerning lymph node manifestations.

**Keywords** Image fusion · Single photon emission computed tomography · Computed tomography · Neuroendocrine tumour · Somatostatin receptor scintigraphy

### Introduction

For scintigraphic imaging of neuroendocrine tumours (NET) highly sensitive and specific tracers are available [1–4]. Cross-sectional imaging by single photon emission computed tomography (SPECT) even further increases the already high rate of detection and localisation of NET manifestations by planar somatostatin receptor scintigraphy (SRS) [5, 6]. Computed tomography (CT), another method widely used for imaging NET, provides partly

complementary information to SRS [2, 4, 6–8]. Thus, both modalities are indispensable in the diagnostics of NET. In order to maximise the information in particular regarding accurate topographic assignment of scintigraphically identified lesions, a combined presentation of both modalities in accurate anatomical correspondence is highly desirable [9].

The fusion of anatomic and functional imaging data requires precise alignment of both, commonly referred to as registration, which has been approached using surface-

matching methods [10], external markers [11], and mathematical algorithms based on the comparison of voxel intensity information, e.g., by performing maximisation of mutual information [9, 10, 12]. Owing to the recent introduction of gamma cameras with integrated CT imaging capability, which combine functional and anatomical imaging in one device, the direct acquisition of co-registered images has become possible [13]. Both retrospective image fusion and co-registered image acquisition by hybrid scanners have been found to substantially improve the localisation accuracy and have also had an impact on consecutive therapy [9, 14–17].

The aim of the present study is to compare side-by-side analysis of separate CT and SPECT images and retrospective image fusion with the use of integrated SPECT–CT for the accuracy of lesion localisation in patients diagnosed with NET.

## Patients and methods

### Patients

Twenty-seven patients (16 male, 11 female; age range 40–79 years, mean 58.8 years) diagnosed with a metastasised tumour of the foregut ( $n=10$ ; bronchial system, two; oesophageal, one; pancreas, seven), midgut ( $n=15$ ; terminal ileum) and hindgut ( $n=1$ , rectum) were included in this study. In one case, the primary localisation of the NET was not known. Histology had been obtained by resection ( $n=24$ ), explorative laparotomy ( $n=2$ ) and needle biopsy ( $n=1$ ) from the primaries and/or metastases. The occurrence of NET was proven by immunohistochemical staining.

### Integrated SPECT–CT

An initial SRS study (In-111 octreotide) identified areas with suspiciously increased nuclide uptake in planar whole body images (4, 24 and 48 h after injection in anterior and posterior view). From these areas, additional SPECT images were acquired (abdomen,  $n=27$ ; thorax,  $n=15$ ). All acquisitions were performed with the patient in the supine position, arms crossed in front of the chest for abdominal imaging and alongside the body for SPECT of the thorax. As an imaging device we used a Hawkeye Millennium VG scanner (GE Medical Systems, Waukesha, WI, USA) with a dual-head gamma camera (MEGP collimators, field of view, 540×400 mm, matrix, 128×128) and an integrated rotating X-ray tube (fixed tube current, 2.5 mA and 140 kV, slice thickness, 10 mm, matrix, 128×128, rotation time, 13.5 s, step-and-shoot technique) for attenuation correction. The total acquisition time was 40 min including the initial transmission scan using the

low-dose X-ray tube (9 min/40 cm) and the subsequent SPECT scan (protocol according to Ref. [1]). After iterative reconstruction, the 3D data set was visualised in sagittal, coronal and transaxial slices. Inherent image fusions were generated from the co-registered SPECT and low-dose CT images (Workstation eNtegra 2.5110, GE Medical Systems).

### Computed tomography

Contrast-enhanced high-resolution CT images were acquired from all patients using a LightSpeed 16/Pro 16 helical 16-channel multi-detector CT (GE Medical Systems). In all cases, the time between the CT imaging and the SRS examination was less than 1 week. Scans of the abdomen (27 patients) and chest (15 patients) were performed with the following imaging parameters: collimated slice thickness, 1.25 mm; total detector width, 20 mm; field of view, 50 cm; matrix, 512×512; tube current, 120 kV and 350 mA; rotation time, 0.5 s; table feed, 13.75 mm/gantry rotation; standard reconstruction kernel. All acquisitions were performed with the patient in the supine position with arms up alongside the head and maximum inspiration. All CT scans were i.v. contrast enhanced with 80 ml (4 ml/s) Ultravist 370 (Schering, Berlin, Germany) with the following delays for the respective body regions: chest 60 s; liver 18 and 40 s; entire abdomen 80 s.

### Retrospective image fusion

A customised software system [15] implemented in AVS/Express 5.0 (Advanced Visual Systems, Waltham, MA, USA) was used for retrospective image fusion. Computations were performed on an SGI O2 workstation (Silicon Graphics, Mountain View, CA, USA). Image fusion involved two steps: (1) an initial rigid alignment of both images was found manually based on triplanar reformatted images; (2) a rigid registration (six degrees of freedom: three translations, three rotations) was computed using an automatic voxel-based technique based on normalised mutual information.

After registration, the co-registered images were visualised in coronal and transaxial planes. All registrations were subject to visual plausibility control, using the body outline and physiological uptake in organs (e.g., liver, spleen, kidney) as a reference. Any registration not regarded as plausible was excluded from further analysis.

The preferred mode of visualisation for this study is 2D image overlay of the colour-coded partially transparent SPECT image data onto CT images, which were displayed in grey levels and windowed for either soft tissue, lung or bone. The fused images were printed on a colour printer, either as transparencies or as paper hard copies.

## Analysis

Three sets of images per patient were read out separately in randomised order by two observers [one nuclear medicine specialist (H.A.) and one experienced radiologist (T.D.)] in consensus: (1) a side-by-side analysis of SPECT and high-resolution CT; (2) retrospectively fused CT and SPECT; and (3) SPECT–CT images acquired by the hybrid camera. The observers were given each set separately, blinded to the results of corresponding sets of images from the two other methods for the same case. Lesions judged as NET manifestations were documented and their localisation was recorded. For comparison of the fusion methods, only those foci of tracer accumulation were enrolled in the analysis which were later confirmed as tumours by either surgery, biopsy, or imaging during clinical follow-up (greater than 6 months with plausible and reproducible morphologic correlation in CT and/or persistently increased tracer accumulation on SRS). The anatomical localisation of focal nuclide uptake classified as pathological in SPECT imaging was reproduced on the CT scans in either fusion method. The reliability of topographic localisation of each focus in either fused image was then assigned a binary rating: 1 for reliable localisation, 0 for cannot be reliably located.

## Results

### Image processing

The generation of fused images was less time consuming for the inherent fusion by integrated SPECT–CT (less than 1 min), compared with that for retrospective image fusion (approximately 25 min including data transfer). In two patients with abdominal SPECT, the retrospective fusion

did not pass plausibility control owing to obvious misregistrations in several attempts, presumably caused by excessive non-rigid motion. These patients were not included in the further analysis.

### Image analysis

In the remaining 25 patients, a total of 87 foci were classified as pathological by SPECT imaging (Table 1). The accuracy of reliable topographic localisation varied between different anatomic regions as described in detail in the following paragraphs.

### Skeleton

Side-by-side analysis and retrospectively fused images achieved an accuracy of 100% (21/21) for the correct classification of bone metastases owing to the structural information on bone lesions derived from multi-detector CT. In SPECT–CT, only 95% (20/21) of foci were correctly localised, as one vertebral lesion was projected into the spinal canal. The low-dose CT was unable to visualise the osteodestruction, whereas multi-detector CT showed evidence of an osteodestruction in the 12th thoracic vertebrae, located peduncular with no extent of tumour into the spinal canal.

### Liver

The retrospective fusion method was limited in areas which were subject to respiratory motion. This was particularly true for hepatic manifestations. Out of 32 foci, two could not be reliably assigned to the liver parenchyma. This was

**Table 1** Reliability of the topographic correspondence assigned to pathological findings using either fusion method.

Localisation of neuroendocrine tumour manifestations	Number	Side-by-side analysis of single photon emission computed tomography (SPECT) and high-resolution computed tomography (CT)		SPECT with integrated low dose CT		Retrospective fusion of SPECT and high-resolution CT	
Liver	32	30/32	96.8% (60/62)	32/32	96.8% (60/62)	30/32	96.8% (60/62)
Bone	21	21/21		20/21		21/21	
Pancreas	5	5/5		4/5		5/5	
Lung	2	2/2		2/2		2/2	
Adrenal glands	1	1/1		1/1		1/1	
Rectum	1	1/1		1/1		1/1	
Mediastinal lymph nodes	8	5/8	62.5%	7/8	87.5%	7/8	87.5%
intra-peritoneal lymph nodes	6	4/6	66.7%	4/6	66.7%	5/6	83.3%
Retroperitoneal and pelvic lymph nodes	11	6/11	54.5%	8/11	72.2%	10/11	90.9%
Total	87	75/87	86.2%	79/87	90.8%	82/87	94.3%

due to different respiratory positions of the patient during multi-detector CT and SPECT imaging. Similar results were observed in the side-by-side analysis. All hepatic foci ( $n=32$ ) were assigned correctly using SPECT-CT (Fig. 1).

Owing to the relatively intense physiological hepatic tracer uptake, the liver silhouette can be easily identified in SPECT images, leading to a classification accuracy of 81% (26/32) of the segmental assignment of hepatic foci. Retrospectively fused images revealed no improvement of segmental assignment. This was largely due to a different respiratory position during CT imaging as compared with the SPECT acquisition. The uncertainty of localisation was in particular observed in cases where the contrast-enhanced CT did not visualise the lesion combined with a shift of the focus outside the segment delineation on fused images ( $n=4$ ), or if the distance between the focus and the morphologic lesion was too large for reliable assignment (two foci were projected outside the liver). While hybrid SPECT-CT in principle allowed for an approximate segmental assignment of foci (accuracy 91%, 29/32), its low-resolution CT component allows neither the visualisation of the hepatic lesion nor the exact definition of liver segments, since intrahepatic vessels are not visible.

#### Abdominal lymph nodes

Abdominal lymph node metastases with focal tracer accumulation ( $n=17$ ) were divided in regions potentially prone to peristaltic movement (intraperitoneal lymph node manifestations,  $n=6$ ) and regions which are less likely to move during or between image acquisitions (pelvic and retroperitoneal lymph nodes:  $n=11$ ).

While a regional topographic assignment of foci was possible using side-by-side analysis or hybrid SPECT-CT in 17/17 cases, the reliable identification as lymph node manifestations was limited (10/17 and 12/17 cases, respectively). The main limitation for the side-by-side analysis was the low background uptake in the mid and lower

abdomen, which led to the uncertainty of focus assignment when instead of a clear tumour manifestation CT showed only unspecific enlarged lymph nodes.

In SPECT-CT one focus was projected partly into the abdominal wall. Retrospective fusion located the same focus precisely onto a non-specific enlarged intestinal lymph node in the lower right quadrant, which proved to be a NET metastasis (Fig. 2). The remaining four foci (three mesenteric and one retroperitoneal manifestations), which could not be reliably located using SPECT-CT, were seen in the upper abdomen where the assignment to candidate structures (pancreas, liver, adrenal glands, bowel wall and lymph nodes) was not clear owing to artefacts from motion and blurring in the low-dose CT images. The assignment of pelvic lymph nodes was successful (2/2) using SPECT-CT (Fig. 3).

Retrospective fusion correctly identified 15 out of 17 findings as lymph node manifestations. The two foci that were not reliably projected onto a candidate structure (morphologically not suspicious) were located in the upper abdomen, making breathing artefacts responsible for misregistrations. Concerning intraperitoneal lymphatic manifestations, CT showed conclusive superposition of foci and enlarged lymph nodes, or projection of foci close to definite tumour masses seen in CT.

#### Other locations

For lesions in the lung and adrenal glands ( $n=3$ ) topographic assignment was equally accurate in all fusion methods. The two pulmonary metastases were correctly localised apically in the upper right lobe and the lingula, respectively, in both fusion methods.

Four primary tumours and one recurrent tumour of the pancreas were seen as focal tracer accumulation in the SPECT images. Of these, one focus could not be reliably assigned to the pancreatic region using SPECT-CT, while retrospective fusion correctly projected five out of five foci

**Fig. 1** Correct assignment of a somatostatin receptor positive lesion to segment 7 of the liver in single photon emission computed tomography with integrated low dose computed tomography (SPECT-CT) (a) and retrospective image fusion of SPECT with high-resolution CT (b).

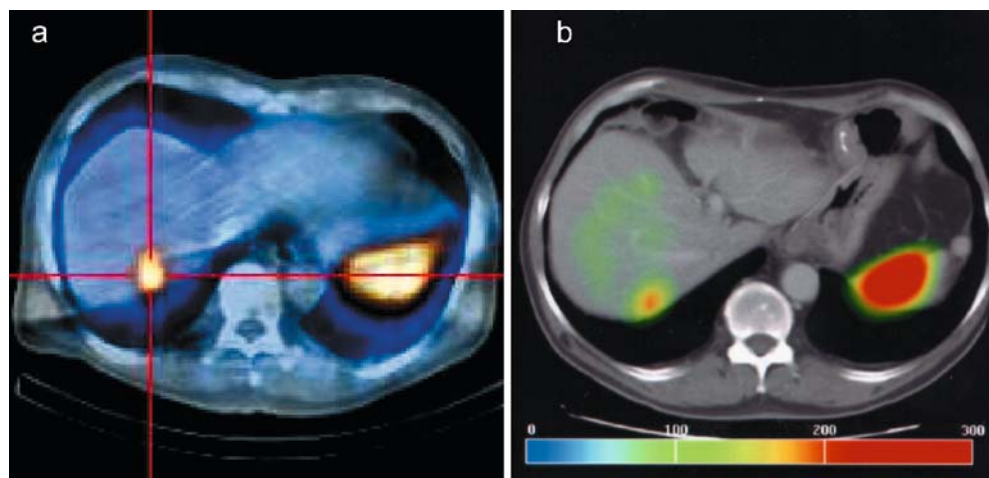
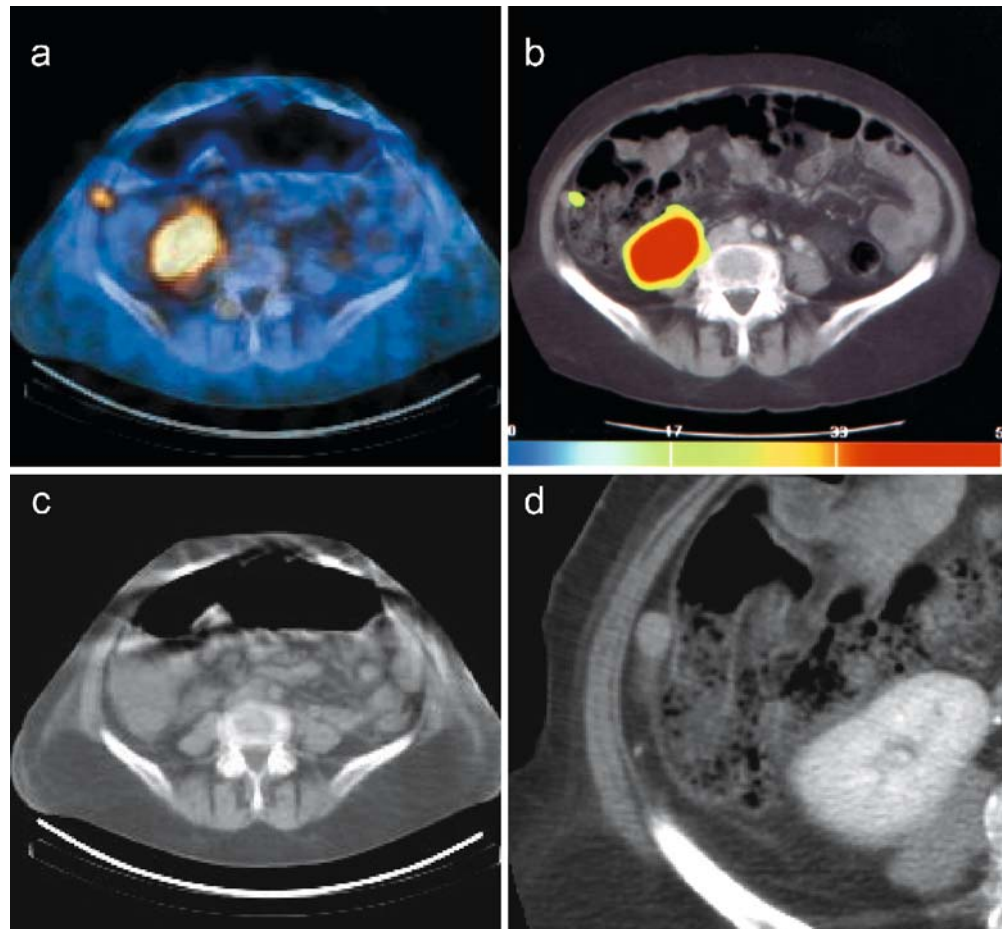


**Fig. 2** Regionally correct focus assignment in both integrated SPECT-CT (a) and retrospective image fusion (b). Because of limited spatial resolution and artefacts from the air-filled bowel, the integrated low-dose CT device does not visualise the corresponding morphologic structure (c). High-resolution CT, however, shows an enlarged contrast-enhancing nodule as the source of the scintigraphic focus, making the diagnosis of an intestinal lymph node metastasis straightforward (d).



onto the corresponding pancreatic lesion seen in contrast-enhanced multi-detector CT. In the side-by-side analysis, this was possible as well, because the lesions seen in CT were the most probable source of increased tracer accumulation. In contrast to multi-detector CT, differentiation

of the pancreas from adjacent structures, like the duodenum and lymph nodes, was not possible in the low-dose CT owing to the limited spatial resolution.

There was one primary NET located in the rectum (Fig. 3). The assignment of the focus was correct in all

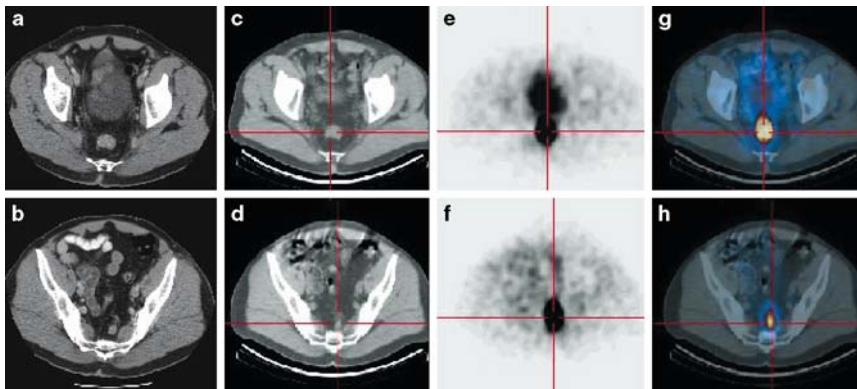


**Fig. 3** Patient with a primary neuroendocrine tumour of the rectum (a contrast-enhancing rectal mass on high-resolution CT) and locoregional lymph node metastasis (b nodular presacral structure on high-resolution CT). Without artefacts due to intra-intestinal air or contrast media, the low-dose CT of the integrated SPECT-CT

achieves satisfactory spatial resolution (c, d primary and lymph node metastasis visualised on low-dose CT. e-h Accurate assignment of foci to the corresponding morphologic structures on integrated SPECT-CT.

fusion modalities. The resolution of the low-dose CT was sufficient to demonstrate a thickening of the rectal wall as a morphologic correlate.

When applied to mediastinal manifestations, retrospective fusion and SPECT–CT were judged as equally successful (accuracy 87.5%) while side-by-side analysis was correct in 63% of cases. The two fusion modalities correctly localised seven out of eight foci. One focus, which was not morphologically suspicious and which was located close to the diaphragm and thus prone to motion artefacts by breathing excursions, was missed by all methods.

## Discussion

The present study compares two methods of image fusion with each other and with side-by-side analysis of SPECT and CT for the purpose of anatomic localisation of scintigraphic foci in SRS. One fusion method is based on retrospective rigid fusion of SPECT with CT data in diagnostic quality acquired with a dedicated separate 16-channel CT scanner. The second fusion approach is an inherent image fusion of SPECT with simultaneously acquired low-dose CT data, obtained from a rotating X-ray tube integrated into the SPECT camera for attenuation measurement and correction.

Compared with the side-by-side analysis, both retrospective fusion and co-registered SPECT–CT showed superior overall accuracies in localising scintigraphic foci (86 versus 94 and 91%, respectively). The lower accuracy of side-by-side analysis is consistent with the data available in the literature, as it appears to be less reliable if no clear candidate lesion is demonstrated by the corresponding morphological modality [18]. In the present study, side-by-side analysis achieved lower accuracy in particular for mediastinal and retroperitoneal lymph node manifestations, where some lesions were not clearly visualised as tumour manifestations in the high-resolution CT.

However, retrospective registration methods as used in the present study are subject to certain limitations. The time interval between the examinations and repositioning of the patient is crucial since anatomical changes caused by organ movement and positioning cannot be compensated by rigid image fusion methods. This represents one of the fundamental problems of retrospective image fusion, which in our study resulted in two major misregistrations and must be considered a possible reason for incorrect assignment of foci. The accuracy of retrospective fusion can be greatly improved when acquiring both images to be registered with precisely the same patient position [12]. Another promising approach to overcome these problems is non-rigid image fusion, a technique which is still under development for application to examinations of the thorax and abdomen [19].

For SPECT–CT no patient repositioning is required. The effects of changes of intestinal filling are also mini-

mised. One advantage of hybrid SPECT–CT imaging is therefore the optimal superposition of functional and anatomical presentations of deforming structures such as the spine, thorax, and the abdominal wall [20].

Aside from patient positioning, respiratory motion affects the quality of fused images. Diagnostic CT images are usually acquired in end-inspiration breath hold. Owing to the long acquisition time of SPECT, breath hold is not feasible for this modality. In the absence of effective gating devices, the resulting SPECT images are a superposition of respiratory states, and therefore represent more of a central respiratory position. Likewise, acquisition of the integrated low-dose CT takes 9 min. Owing to the resulting blurring of moving structures, it is more similar to SPECT than to an external diagnostic CT. The present study showed minor inaccuracies of the retrospective fusion for liver lesions regarding the assignment to hepatic segments. By showing morphological correlatives as “candidate structures” in dedicated CT, however, a reliable assignment of foci is usually still possible. To improve retrospective fusion, the CT acquisition could be performed in the medial respiratory position, in order to minimise localisation uncertainty in areas with substantial respiratory motion. Goerres et al. [21] have described such an approach for integrated PET–CT acquisition.

An important disadvantage of the SPECT–CT system used in the present study is the limited spatial resolution and tissue contrast of the integrated low-dose CT, which is in fact merely an advanced attenuation map [13]. Today this is accepted as inevitable in order to minimise radiation exposure, although SPECT cameras with integrated dedicated CT scanners have recently become available. In addition, the long duration of the acquisition causes respiratory and peristaltic motion artefacts. When localising foci in well-presented structures such as the liver (size), bones (tissue density contrast), or adrenal glands (characteristic position), these problems can be minimised, as is illustrated by our results. The assignment of findings to the aforementioned organs was almost equally reliable using both fusion methods.

A particular challenge for the SPECT–CT used in our study is the localisation of abdominal foci that correspond to mesenteric or retroperitoneal lymph nodes, since these usually show only minimal volume increase. Furthermore, the low-dose CT component is more susceptible to artefacts created by intra-intestinal air or contrast. This is reflected by 29% uncertain assignments of foci to abdominal lymph node metastases in the present study.

In summary, we found that both image fusion methods were equally well suited for the localisation of SRS foci in parenchymal organs. Concerning the overall accuracy of focus assignment, both are superior to side-by-side analysis. The topographic assignment of SPECT findings using hybrid SPECT–CT was satisfactory, while requiring only a fraction of the logistic effort and time necessary for the retrospective approach. The latter was not consistently

successful in providing valid image fusions. However, for the identification of intra-abdominal lymph node manifestations retrospective fusion was superior, mostly owing to the substantially better spatial resolution of diagnostic CT scanners.

## References

- Krenning EP, Kwekkeboom DJ, Bakker WH, Breeman WA, Kooij PP, Oei HY, van Hagen M, Postema PT, de Jong M, Reubi JC et al (1993) Somatostatin receptor scintigraphy with [<sup>111</sup>In-DTPA-D-Phe<sup>1</sup>]- and [<sup>123</sup>I-Tyr<sup>3</sup>]-octreotide: the Rotterdam experience with more than 1,000 patients. *Eur J Nucl Med* 20(8):716–731
- Lebtahi R, Cadiot G, Sarda L, Daou D, Faraggi M, Petegnief Y, Mignon M, le Guludec D (1997) Clinical impact of somatostatin receptor scintigraphy in the management of patients with neuroendocrine gastroenteropancreatic tumors. *J Nucl Med* 38(6):853–858
- Chiti A, Briganti V, Fanti S, Monetti N, Masi R, Bombardieri E (2000) Results and potential of somatostatin receptor imaging in gastroenteropancreatic tract tumours. *Q J Nucl Med* 44(1):42–49
- Ricke J, Klose KJ, Mignon M, Oberg K, Wiedenmann B (2001) Standardisation of imaging in neuroendocrine tumours: results of a European delphi process. *Eur J Radiol* 37(1):8–17
- Schillaci O, Scopinaro F, Danieli R, Angeletti S, Tavolaro R, Annibale B, Cannas P, Marignani M, Colella AC, Delle Fave G (1997) Single photon emission computerized tomography increases the sensitivity of indium-111-pentetreotide scintigraphy in detecting abdominal carcinoids. *Anticancer Res* 17(3B):1753–1756
- Schillaci O, Spanu A, Scopinaro F, Falchi A, Danieli R, Marongiu P, Pisu N, Madeddu G, Delle Fave G, Madeddu G (2003) Somatostatin receptor scintigraphy in liver metastasis detection from gastroenteropancreatic neuroendocrine tumors. *J Nucl Med* 44(3):359–368
- Gotthardt M, Dirkmorfeld LM, Wied MU, Rinke A, Behe MP, Schlieck A, Hoffken H, Alfke H, Joseph K, Klose KJ, Behr TM, Arnold R (2003) Influence of somatostatin receptor scintigraphy and CT/MRI on the clinical management of patients with gastrointestinal neuroendocrine tumors: an analysis in 188 patients. *Digestion* 68(2–3):80–85
- Chiti A, Fanti S, Savelli G, Romeo A, Bellanova B, Rodari M, van Graafeiland BJ, Monetti N, Bombardieri E (1998) Comparison of somatostatin receptor imaging, computed tomography and ultrasound in the clinical management of neuroendocrine gastro-entero-pancreatic tumours. *Eur J Nucl Med* 25(10):1396–1403
- Amthauer H, Ruf J, Bohmig M, Lopez-Hanninen E, Rohlfing T, Wernecke KD, Plockinger U, Gutberlet M, Lemke AJ, Steinmuller T, Wiedenmann B, Felix R (2004) Diagnosis of neuroendocrine tumours by retrospective image fusion: is there a benefit? *Eur J Nucl Med Mol Imaging* 31(3):342–348
- West JB, Fitzpatrick JM, Wang MY, Dawant BM, Maurer CR, Kessler RM, Maciunas RJ (1999) Retrospective intermodality registration techniques for images of the head: surface-based versus volume-based. *IEEE Trans Med Imag* 18(2):144–150
- Tomura N, Watanabe O, Omachi K, Sakuma I, Takahashi S, Otani T, Kidani H, Watarai J (2004) Image fusion of thallium-201 SPECT and MR imaging for the assessment of recurrent head and neck tumors following flap reconstructive surgery. *Eur Radiol* 14(7):1249–1254
- Lemke AJ, Niehues SM, Hosten N, Amthauer H, Boehmig M, Stroszczynski C, Rohlfing T, Rosewicz S, Felix R (2004) Retrospective digital image fusion of multidetector CT and <sup>18</sup>F-FDG PET: clinical value in pancreatic lesions—a prospective study with 104 patients. *J Nucl Med* 45(8):1279–1286
- Bocher M, Balan A, Krausz Y, Shrem Y, Lonn A, Wilk M, Chisin R (2000) Gamma camera-mounted anatomical X-ray tomography: technology, system characteristics and first images. *Eur J Nucl Med* 27(6):619–627
- Even-Sapir E, Keidar Z, Sachs J, Engel A, Bettman L, Gaitini D, Guralnik L, Werbin N, Iosilevsky G, Israel O (2001) The new technology of combined transmission and emission tomography in evaluation of endocrine neoplasms. *J Nucl Med* 42(7):998–1004
- Hosten N, Kreissig R, Puls R, Amthauer H, Beier J, Rohlfing T, Stroszczynski C, Herbel A, Lemke AJ, Felix R (2000) Fusion of CT and PET data: methods and clinical relevance for planning laser-induced thermotherapy of liver metastases. *Rofo* 172(7):630–635
- Krausz Y, Keidar Z, Kogan I, Even-Sapir E, Bar-Shalom R, Engel A, Rubinstein R, Sachs J, Bocher M, Agranovicz S, Chisin R, Israel O (2003) SPECT/CT hybrid imaging with <sup>111</sup>In-pentetreotide in assessment of neuroendocrine tumours. *Clin Endocrinol* 59(5):565–573
- Schillaci O, Danieli R, Manni C, Simonetti G (2004) Is SPECT/CT with a hybrid camera useful to improve scintigraphic imaging interpretation? *Nucl Med Commun* 25(7):705–710
- Israel O, Keidar Z, Iosilevsky G, Bettman L, Sachs J, Frenkel A (2001) The fusion of anatomic and physiologic imaging in the management of patients with cancer. *Semin Nucl Med* 31:191–205
- Slomka PJ, Dey D, Przetak C, Aladl UE, Baum RP (2003) Automated 3-dimensional registration of stand-alone (<sup>18</sup>F)-FDG whole-body PET with CT. *J Nucl Med* 44(7):1156–1167
- Patton JA, Delbeke D, Sandler MP (2000) Image fusion using an integrated, dual-head coincidence camera with x-ray tube-based attenuation maps. *J Nucl Med* 41:1364–1368
- Goerres GW, Burger C, Schwitter MW, Heidelberg TN, Seifert B, Von Schulthess GW (2003) PET/CT of the abdomen: optimizing the patient breathing pattern. *Eur Radiol* 13(4):734–739